Volume 1 | Number 1 | Jan 2013 | Pages 1–100

PCCP

Physical Chemistry Chemical Physics
www.rsc.org/pccp

ROYAL SOCIETY OF CHEMISTRY

ROYAL SOCIETY OF CHEMISTRY

www.rsc.org/pccp

PCCP

PAPER

Optimization of second harmonic generation of gold nanospheres and nanorods in aqueous solution: the dominant role of surface area†

Hoang Minh Ngo,[a] Phuong Phong Nguyen[b] and Isabelle Ledoux-Rak[*a]

Size and shape of gold nanoparticles (AuNPs) have a strong influence on their second order nonlinear optical properties. In this work, we propose a systematic investigation of surface and shape effects in the case of small gold nanoparticles. Colloidal solutions on AuNPs with different sizes and shapes have been synthesized, i.e. nanospheres (diameters 3.0; 11.6; 15.8; 17.4; 20.0 and 43 nm) and nanorods (aspect ratios 1.47; 1.63 and 2.30). The first hyperpolarizability β values of these AuNPs have been measured by Harmonic Light Scattering (HLS) at 1064 nm. For nanospheres and nanorods, we found that their β values are governed by a purely local, dipolar contribution, as confirmed by their surface area dependence. As an important consequence of these surface effects, we have revisited the previously reported aspect ratio dependence of β values for gold nanorods, and evidenced the predominant influence of nanoparticle area over aspect ratio considerations.

Introduction

Gold nanoparticles (AuNPs) are currently investigated for a wide range of applications, such as photonics, information storage, electronic and optical detection systems, therapeutics, diagnostics, photovoltaic, and catalysis.[1–11] The size and shape of AuNPs affect significantly their physical and chemical properties, especially their linear and nonlinear optical response. Many investigations have been focused on controlling the size and shape of AuNPs, with various synthesis conditions and methods for nanospheres,[12,13] nanorods,[14–22] nanostars,[23,24] nanoflowers[25] and so on.

The quadratic nonlinear optical properties of AuNPs are generally defined by their hyperpolarizability β values. The Harmonic Light Scattering[26,27] (HLS) technique is used for the determination of the first hyperpolarizability tensor β of nanoparticles in colloidal solution. The β values depend on size, shape, material and crystal structure, etc. As a result, large magnitudes of AuNPs hyperpolarizability have been reported.[17,18,28–31]

In this work we propose a systematic investigation of the influence of the AuNP surface area on their β values. Previous reports evidenced a fourth-power dependence of the HLS intensity with respect to nanosphere diameters,[32] but no quantitative hyperpolarizability values have been systematically provided for a large range of surface areas. Here we will explore the effect of surface area on Au nanospheres with diameters ranging from 3 to 80 nm, in order to reach the upper as well as the lower limit of validity of the purely dipolar origin of β values. Moreover, by studying gold nanorods with different surface areas, we will evidence the predominance of these surface effects over shape factors, leading us to revisit previous studies on the NLO properties of these nanorods.[17] The fundamental wavelength is 1064 nm, significantly higher than that chosen in Ref. 32, allowing to measure β values with a strong plasmon resonance enhancement at the harmonic frequency. In our case, the accuracy on β values (+/- 15%) is slightly better than in ref. 32 (+/- 20%).

Materials and methods

Materials

Principle: AuNP synthesis is based on one of these two standard reactions:

$$AuCl_4^- + BH_4^- + 3H_2O \rightarrow Au + BO_3^- + 4Cl^- + 5H^+ + H_2$$

(reduction by BH_4^-, for small particles and seeds).

$$2AuCl_4^- + 3C_6H_8O_6 \rightarrow 2Au + 8Cl^- + 3C_6H_6O_6 + 6H^+$$

(reduction by ascorbic acid, for larger particles)
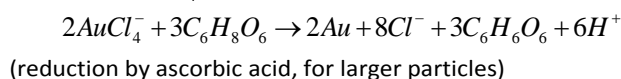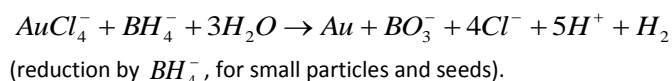
Actually, these reactions are very fast and their equilibrium constants K are very large, so the reaction process is complete, eliminating the $AuCl_4^-$ ions after syntheses.

Tetrachloroauric(III) acid trihydrate (HAuCl₄.3H₂O), ascorbic acid (C₆H₈O₆), tri-sodium citrate (C₆H₅Na₃O₇.2H₂O), silver nitrate (AgNO₃, 99%), sodium borohydride (NaBH₄, 99.99%),

[a] Laboratoire de Photonique Quantique et Moléculaire, UMR 8537, Ecole Normale Supérieure de Cachan, CentraleSupélec, CNRS, Université Paris-Saclay, 94235 Cachan, France. E-mail: ledoux@lpqm.ens-cachan.fr
[b] Department of Chemistry, University of Science, Vietnam National University, Ho Chi Minh City, Vietnam
† Electronic Supplementary Information (ESI) available: characterization of nanoparticles such as analysis of the UV-Vis absorbance spectra, the measurement of SHG from AuNPs; nonlinear optical (NLO) properties of various AuNPs. See DOI: 10.1039/x0xx00000x

This journal is © The Royal Society of Chemistry 20xx

Phys. Chem. Chem. Phys., 2015, 00, 0-0 | 1

hexadecyltrimethylammonium bromide (CTAB, $C_{19}H_{42}BrN$ 99%), polyvinylpyrrolidone (PVP; 40,000 g/mol), poly(vinyl alcohol) (PVA; 40,000 g/mol) and gold nanospheres (size ~ 80 nm) were purchased from Sigma-Aldrich. The solutions were prepared using ultra-pure water from a Millipore system (18 MΩ cm-1) throughout the experiment. All aqueous samples are at neutral pH=7.

Synthesis of different shapes of gold nanoparticles

Gold nanospheres (AuNSs):

Small-size AuNSs (3.0nm): A 20 mL aqueous solution containing 1.45×10^{-4} M $HAuCl_4$ and 5×10^{-4} M tri-sodium citrate was prepared. Next, 0.3 mL of 0.01 M $NaBH_4$ solution was quickly added to the solution while stirring. The solution turned pink immediately after adding $NaBH_4$, indicating particle formation.

Medium-size AuNSs (11.6; 15.8; 17.4 and 20.0 nm): In the typical synthesis, different protective agents (PVA, PVP) were dissolved in 20 mL H_2O Millipore under stirring. After the complete dissolution of the protective agent, $HAuCl_4$ 0.029 M was added, the solution being stirred for 5 min. Then, an aqueous solution of ascorbic acid 0.1 M was added into the liquid. The colour of solution slowly changed from white to red.

The seed-mediated growth method is so far the most popular method for the synthesis of colloidal Au large-size nanospheres and nanorods. This technique is implemented according to a two-step procedure.[12–16,33–35]

Seed solution: The first step consists in the preparation of gold spherical nanoparticle seeds. This preparation was performed starting from a 10 mL aqueous solution of CTAB 0.1 M. Then, 0.1 mL $HAuCl_4$ 0.029 M was added under stirring. After that, 0.15 mL $NaBH_4$ 0.01 M was then slowly added. The seed solution was kept for various durations (0.5, 1 h) before being used. This solution was then used as the seeding solution for the growth of the nanorods and large-size nanospheres.

Larger-size AuNSs (43 nm): In the second step, 10 mL of growth solution, containing 1.45×10^{-4} M $HAuCl_4$ and 0.025 M CTAB, was mixed with a 0.055 mL of 0.1 M freshly prepared ascorbic acid solution. Next (after 1 h), 0.02 mL of the seed solution was added and stirred. Within 5-10 min, the solution color changed to deep red.

Gold nanorods (AuNRs):

0.1 mL $HAuCl_4$ 0.029 M and 0.075 mL $AgNO_3$ 0.01 M were added to a 10 mL aqueous solution of CTAB 0.025 M, the growth solution changed to bright yellow. Then, 0.055 mL ascorbic acid 0.1M was added and the growth solution became colorless. At that time, 12 μl (0.5 h, 1 h) and 24 μl (1 h) of the seed solution were added quickly to the growth solution. The colour of growth solution immediately changed from white to dark blue. The solution contained respectively 1.47; 1.63 and 2.30 aspect ratio (*AR*) nanorods.

Results and Discussion

Transmission Electron Microscopy is the best tool to investigate the morphology and size distribution of nanoscale objects. Samples for TEM were prepared by dropping a gold colloidal solution onto a carbon-coated Cu grid, followed by slow evaporation of solvent at room temperature. Figure 1 and 2 show TEM images of different average diameters (AuNSs) and *AR* (AuNRs), which are consistent with the results of the analysis of UV-Vis (Figure S1, Figure S2 and Table S1 in the Supporting Information). The average particles sizes are obtained by measuring and averaging diameters for about 100 particles.

AuNS 1, d = 3.0 ± 0.5 nm   AuNS 2, d = 11.6 ± 1.0 nm

AuNS 3, d = 15.8 ± 1.1 nm   AuNS 4, d = 17.4 ± 1.5 nm

AuNS 5, d = 20.0 ± 1.2 nm   AuNS 6, d = 43.0 ± 2.5 nm
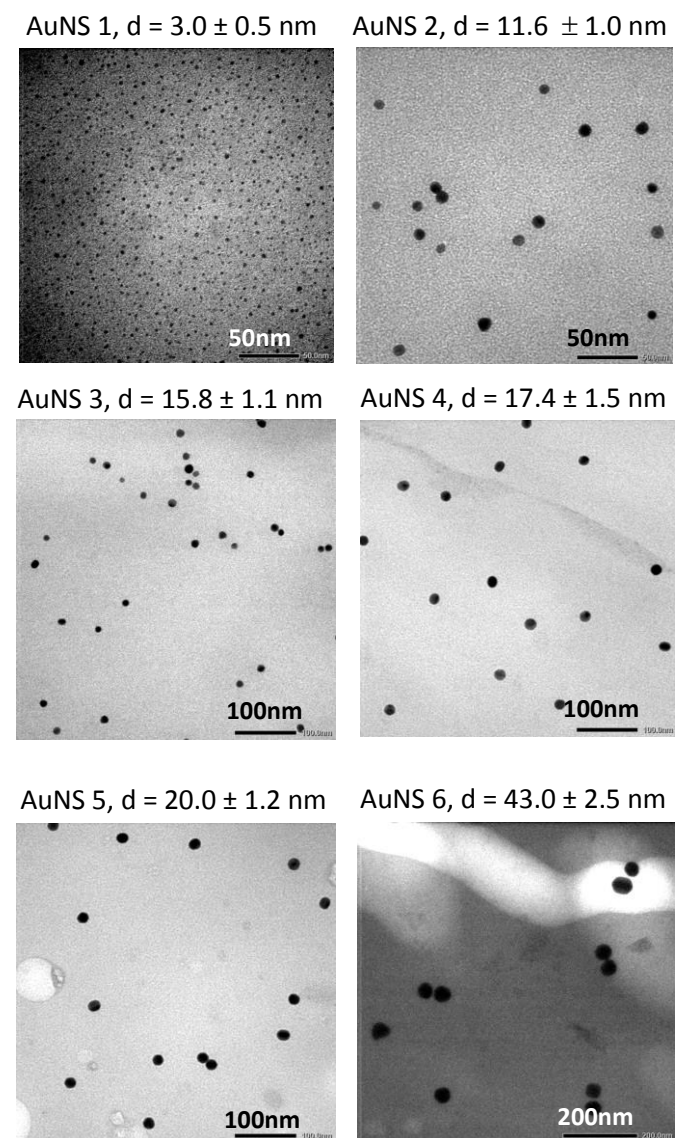
Fig. 1 TEM image and size of AuNSs. d is diameter of nanospheres.

2 | *Phys. Chem. Chem. Phys.,* 2015, **00**, 0-0

This journal is © The Royal Society of Chemistry 20xx

AuNR 1, *AR* = 1.47

AuNR 2, *AR* = 1.63

50nm

100nm

AuNR 3, *AR* = 2.30

50nm
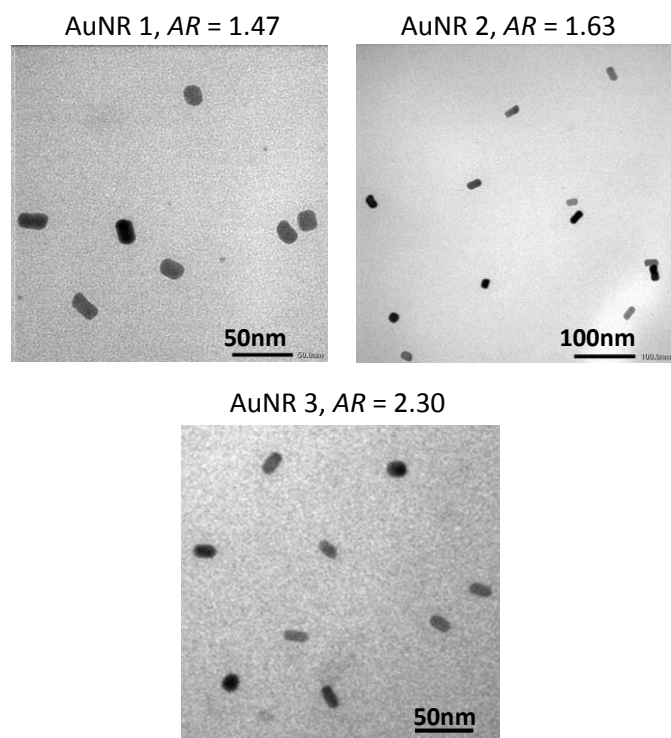
Fig. 2 TEM image of AuNRs with different ARs.

Freshly prepared water solutions of AuNPs were characterized by HLS at 1.064 µm for the determination of their first order hyperpolarizability, on the basis of a known β value (β_{H2O} = 0.055 × 10^{-30} esu)[17] of the water solvent used as a reference. Different concentrations were used for each kind of particle. As β values are independent on particle concentrations, aggregation effects can be ruled-out.

As proposed by other authors,[18,28–31] from these β values, the β values per gold atom, i.e. β', have been calculated according to the relation[29,36,37]

$$\beta = \frac{\beta'}{\sqrt{N}},$$

where N is the number of atoms per nanoparticle. This relation is valid for a centrosymmetric assembly (e.g. a nanoparticle[36] or a dendrimer[37]) of N individual objects (molecules, or atoms in the present case).

For this purpose, the volume of the AuNPs must be determined. Particle concentration is calculated from the known concentration of the initial gold solution, and from the average volume of nanoparticles. The concentration of the reducing agent used for the reaction was always higher than the minimal reducing agent concentrations required to achieve a total reaction. It means that reduction of Au^{+III} species to atomic Au^0 is complete, and thereby only gold nanoparticles were formed.

The β per particle is determined from HLS measurements by using the equation:

$$\frac{P}{P_0} = \frac{\left[N_{nanoparticles}\left\langle\beta^2_{nanoparticles}\right\rangle + N_{H_2O}\left\langle\beta^2_{H_2O}\right\rangle\right]}{N_{H_2O}\left\langle\beta^2_{H_2O}\right\rangle}$$

where $N_{nanoparticles}$, $\beta_{nanoparticles}$ and P are respectively the concentration of the nanoparticles, the first hyperpolarizability and the slope of the HLS intensity recorded from nanoparticle solutions, N_{H2O}, β_{H2O} and P_0 are respectively the concentration of the water, the first hyperpolarizability and the slope of the HLS intensity recorded from pure water. All values are presented in Table 1 (See also Table S2 in the Supporting Information).

Table 1 The first hyperpolarizability of Au per atom (β') and per particle (β). For AuNRs, L is the length and W the diameter of the rods. The relative experimental error on β is ± 15%, mainly due to the uncertainly from HLS measurements in water, the signal/noise ratio for the SHG signal being much lower in this case than for AuNPs solutions

Sample	Diameter (nm)	Surface area (nm²)	β per particle (β) (10^{-26}) esu	β per atom (β') (10^{-30}) esu	β_R (10^{-20}) esu
AuNS 1	3.0 ± 0.5	30	0.4	130	1
AuNS 2	11.6 ± 1.0	420	3.4	160	0.56
AuNS 3	15.8 ± 1.1	780	6.5	190	0.57
AuNS 4	17.4 ± 1.5	950	8.3	210	0.61
AuNS 5	20.0 ± 1.2 / AR = 1.0	1300	13.0	270	0.72
AuNS 6	43.0 ± 2.5	5800	58.0	370	0.69
AuNS 7*	80.0 ± 3.0	20100	260.0	660	0.9
AuNR 1	20.6 ± 2.1 (L) - 14.0 ± 1.3 (W) / *AR* = 1.47	1200	6.6	150	
AuNR 2	20.4 ± 2.5 (L) - 12.5 ± 1.2 (W) / *AR* = 1.63	1050	4.7	120	
AuNR 3	20.4 ± 2.0 (L) - 8.9 ± 0.9 (W) / *AR* = 2.30	700	2.9	110	

* Purchased from Sigma-Aldrich

This journal is © The Royal Society of Chemistry 20xx

Phys. Chem. Chem. Phys., 2015, 0-0 | **3**

The increasing β and β' value for AuNSs (from 0.4 to 260 $\times$ 10^{-26} esu and from 130 to 660 $\times$ 10^{-30} esu, respectively) corresponds to the rise in nanoparticle diameter from 3.0 to 80.0 nm. The β values of AuNSs are consistent with those reported by Galletto[30] who published values ranging from 0.6 to 16.6 $\times$ 10^{-26} esu for a particle diameter range of 4.9-22 nm, but at the same fundamental wavelength, after corrections of β value of water.

When further comparing our β and β' values to the results obtained by K. Das[29] *et al.* and Yara *et al.*[38] (800 nm, 150 fs; 784 nm, 150 fs; respectively), for particles with the same size (~20 nm), our results (13.0 $\times$ 10^{-26} esu) are significantly higher than the values obtained by these authors (3.8 $\times$ 10^{-26} esu; 2.7 $\times$ 10^{-26} esu; respectively). It must be pointed-out that our HLS measurements are performed in a strongly resonant regime, the second harmonic wavelength at 532 nm being very close to that of the AuNPs plasmon resonance. On the contrary, measurements reported in ref.[29,38], performed around 800 nm, are much less resonant, the SH wavelength at 400 nm being significantly different from that of the gold plasmon resonance, resulting in smaller β values.
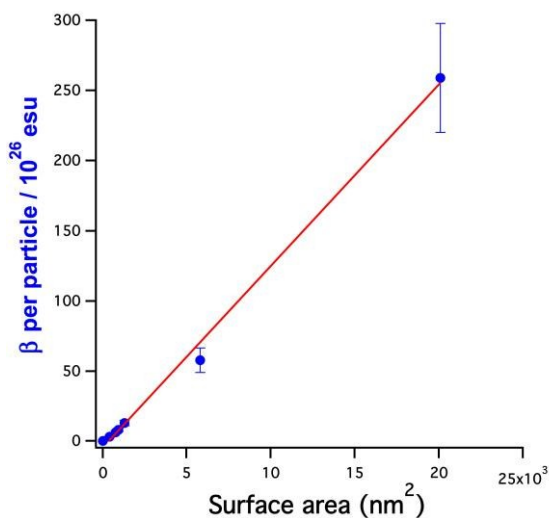
Fig. 3 HLS values of the first hyperpolarizability (β) per Au particle in water solution as a function of the surface area of AuNSs. The red line is a least-square linear fit of β with respect to surface area.

In Figure 3, these results emphasize the strong dependence of the first hyperpolarisability of AuNPs on the surface area of nanosphere. A linear dependence of β per particle with respect to the surface area of AuNSs is observed, with a remarkable correlation coefficient (0.9962). This confirm that these high β values and their linear increase with particle surface area arise from surface defects of gold nanospheres, leading to centrosymmetry breaking and resulting in a dipolar-type NLO response, as discussed in ref. 39. In this case, the HLS intensity is expected to scale with the fourth power with particle diameter, as confirmed by our results on Figure 3.

It is interesting to go further in hyperpolarizability data analysis by inferring from experimental HLS results a "reduced hyperpolarizability" β_R, which takes into account surface effects and plasmonic local field effects at the fundamental and harmonic frequencies. The β_R can be defined, in a purely dipolar, local regime, as follow[18]:

$$\beta_R = \frac{\beta}{k^2 S f(2\omega)\left(f(\omega)\right)^2}$$

where β is the hyperpolarizability of the nanoparticle as measured by HLS, k is the wave vector of the fundamental wave, S is the surface area of the nanoparticle, $f(\omega)$ and $f(2\omega)$ are the local field factors at the fundamental (ω) and harmonic (2ω) frequencies. In the case of spherical nanoparticles, we can use a simple expression of these local field factors:

$$f(\omega,2\omega) = \left|\varepsilon(\omega,2\omega) + 2\varepsilon_s\right|^{-1}$$

where ε and ε_s are the dielectric constants of gold and of the solvent (water), respectively. This expression is valid for particles having a small diameter as compared to the incident wavelength. We have checked that for even 80 nm− nanospheres, the non-dipolar contribution to the local field factors remains negligible, according to Eq. (1) and (2) of ref. 39. Dielectric constant values of gold nanoparticles are assimilated to the values of bulk gold, an assumption which is expected to be valid for particle diameters higher than 2 nm. These ε values are inferred from the data table published by Johnson and Christy.[40] Calculated β_R values are reported in Table 1. These data illustrate the limit of our approximations at the two extreme values of the diameter range. Whereas β_R remains almost constant (considering the relative experimental errors on β values, around +/- 10%) for most nanospheres (NS2 to NS6), for the smallest value (3 nm), β_R is significantly larger. This depart for the average β_R values is most probably related to the fact that for very small particles, taking bulk values for AuNP dielectric constants is not more valid. On the other extremity, the increased β_R value can reflect the emergence of non-dipolar effects in larger AuNPs.

A significant increase of β per atom and particle with the increase in the *AR* of AuNRs has been previously reported.[17] This result was obtained only when AuNRs displayed the same volume and surface. Here, we report an opposite behavior, β decreasing when increasing *AR*. In this work, the length (~20 nm) of AuNRs is kept constant, whereas the radius decreases when increasing *AR* (Figure 4). When *AR* increases from 1.0 to 2.3, a significant decrease of β (from 13.0 to 2.9 $\times$ 10^{-26} esu) and β' values (from 270 to 110 $\times$ 10^{-30} esu) is observed. However, in our work, the AuNR surface strongly decreases when increasing *AR*'s. Therefore, the role of the AuNR surface overcomes the influence of *AR* observed in ref.[17] for particles having the same surface only.

4 | *Phys. Chem. Chem. Phys.,* 2015, **00**, 0-0

This journal is © The Royal Society of Chemistry 20xx
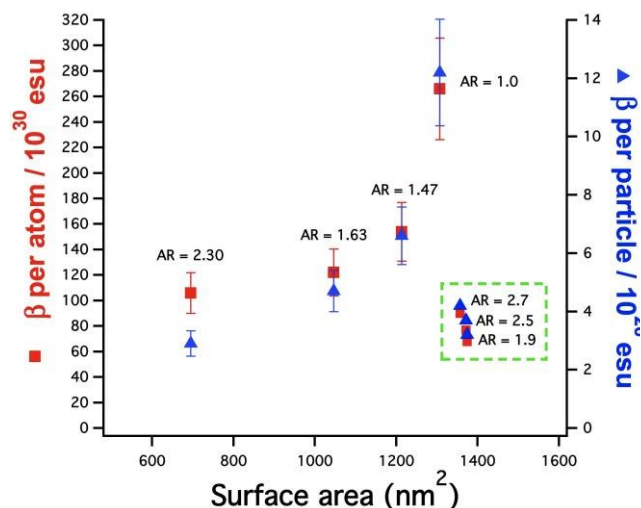
Fig. 4 HLS values of the first hyperpolarizability (β) per Au atom (red squares) and per Au particle (blue triangles) in water solution as a function of the surface area of AuNRs. For comparison, data on AuNRs reported in ref.[17] are presented in the dotted border rectangle.

A confirmation of this hypothesis can be found by comparing, for the same variation ΔAR of AR, the hyperpolarizability changes $\Delta\beta'$ found in this work to those obtained by Anu Singh et al.[17].

For ΔAR = 0.8, the change in β' ($\Delta\beta'$ = $-$ 48 $\times$ 10^{-30} esu) is significantly higher (and of an opposite sign) than the values obtained in ref.[17] ($\Delta\beta'$ = $+$ 22 $\times$ 10^{-30} esu). Ref.[17] results are obtained when the AuNRs have the same surface area while the surface of our AuNRs strongly changes.

In addition in the present work, for almost the same variation of surface area ΔS for AuNRs (ΔS = 500 nm^2 between AuNR1 and AuNR3) and AuNSs (ΔS = 530 nm^2 between NS4 and NS2), $\Delta\beta'$ = 50 $\times$ 10^{-30} esu observed for AuNSs is comparable to $\Delta\beta'$ = 40 $\times$ 10^{-30} esu observed for AuNRs. This change is much higher that the increase of $\Delta\beta'$ ($+$ 22 $\times$ 10^{-30} esu) reported in Ref. 17 for NR having the same surface. This result confirms the major influence of surface area on the value of the first hyperpolarizability of nanoparticles, which dominates the contribution of ΔAR.

Conclusion

We have achieved the synthesis and characterization of AuNPs with different diameters (AuNSs) and AR (AuNRs), which were controlled by varying the protective agent, the reductive agent and by using the seed-mediated method. AuNPs display exceptionally strong β values. We demonstrated that the first hyperpolarizability (β) linearly depends on the surface area of AuNSs. The calculation of a "reduced" β_R value taking into account local field factors and surface effects showed a remarkable constant value for most AuNSs, with departs from this behaviour for very small and large particles as expected from the theory. This predominant influence of surface effects is confirmed by the investigation of the NLO properties of

AuNRs, for which the increase of AR leads to the decrease in β values, due to the change of particle surface areas.

Acknowledgements

Notes and references

1 C. J. Murphy, T. K. Sau, A. M. Gole, C. J. Orendorff, J. Gao, L. Gou, S. E. Hunyadi and T. Li, *J. Phys. Chem. B*, 2005, **109**, 13857–13870.
2 C. Burda, X. Chen, R. Narayanan and M. A. El-Sayed, *Chem. Rev.*, 2005, **105**, 1025–1102.
3 T. K. Sau, A. L. Rogach, F. Jäckel, T. A. Klar and J. Feldmann, *Adv. Mater.*, 2010, **22**, 1805–1825.
4 D. V. Talapin, J.-S. Lee, M. V. Kovalenko and E. V. Shevchenko, *Chem. Rev.*, 2010, **110**, 389–458.
5 B. R. Cuenya, *Thin Solid Films*, 2010, **518**, 3127–3150.
6 M.-C. Daniel and D. Astruc, *Chem. Rev.*, 2004, **104**, 293–346.
7 S. Eustis and M. A. El-Sayed, *Chem. Soc. Rev.*, 2006, **35**, 209–217.
8 R. Sardar, A. M. Funston, P. Mulvaney and R. W. Murray, *Langmuir*, 2009, **25**, 13840–13851.
9 J. Zhou, J. Ralston, R. Sedev and D. A. Beattie, *J. Colloid Interface Sci.*, 2009, **331**, 251–262.
10 N. L. Rosi and C. A. Mirkin, *Chem. Rev.*, 2005, **105**, 1547–1562.
11 D. A. Giljohann, D. S. Seferos, W. L. Daniel, M. D. Massich, P. C. Patel and C. A. Mirkin, *Angew. Chem. Int. Ed Engl.*, 2010, **49**, 3280–3294.
12 N. G. Bastús, J. Comenge and V. Puntes, *Langmuir*, 2011, **27**, 11098–11105.
13 S. D. Perrault and W. C. W. Chan, *J. Am. Chem. Soc.*, 2009, **131**, 17042–17043.
14 B. d. Busbee, S. o. Obare and C. j. Murphy, *Adv. Mater.*, 2003, **15**, 414–416.
15 B. Nikoobakht and M. A. El-Sayed, *Chem. Mater.*, 2003, **15**, 1957–1962.
16 N. R. Jana, L. Gearheart and C. J. Murphy, *J. Phys. Chem. B*, 2001, **105**, 4065–4067.
17 A. Singh, A. Lehoux, H. Remita, J. Zyss and I. Ledoux-Rak, *J. Phys. Chem. Lett.*, 2013, **4**, 3958–3961.
18 Y. El Harfouch, E. Benichou, F. Bertorelle, I. Russier-Antoine, C. Jonin, N. Lascoux and P.-F. Brevet, *J. Phys. Chem. C*, 2014, **118**, 609–616.
19 C. J. Murphy, T. K. Sau, A. Gole and C. J. Orendorff, *MRS Bull.*, 2005, **30**, 349–355.
20 X. Huang, S. Neretina and M. A. El-Sayed, *Adv. Mater.*, 2009, **21**, 4880–4910.
21 J. Pérez-Juste, I. Pastoriza-Santos, L. M. Liz-Marzán and P. Mulvaney, *Coord. Chem. Rev.*, 2005, **249**, 1870–1901.
22 C. J. Murphy, L. B. Thompson, D. J. Chernak, J. A. Yang, S. T. Sivapalan, S. P. Boulos, J. Huang, A. M. Alkilany and P. N. Sisco, *Curr. Opin. Colloid Interface Sci.*, 2011, **16**, 128–134.
23 E. Hao, R. C. Bailey, G. C. Schatz, J. T. Hupp and S. Li, *Nano Lett.*, 2004, **4**, 327–330.
24 C. L. Nehl, H. Liao and J. H. Hafner, *Nano Lett.*, 2006, **6**, 683–688.
25 S. Boca, D. Rugina, A. Pintea, L. Barbu-Tudoran and S. Astilean, *Nanotechnology*, 2011, **22**, 055702.
26 R. W. Terhune, P. D. Maker and C. M. Savage, *Phys. Rev. Lett.*, 1965, **14**, 681–684.

This journal is © The Royal Society of Chemistry 20xx

Phys. Chem. Chem. Phys., 2015, 0-0 | **5**

27 K. Clays and A. Persoons, *Phys. Rev. Lett.*, 1991, **66**, 2980–2983.
28 C. Hubert, L. Billot, P.-M. Adam, R. Bachelot, P. Royer, J. Grand, D. Gindre, K. D. Dorkenoo and A. Fort, *Appl. Phys. Lett.*, 2007, **90**, 181105.
29 K. Das, A. Uppal, R. K. Saini, G. K. Varshney, P. Mondal and P. K. Gupta, *Spectrochim. Acta. A. Mol. Biomol. Spectrosc.*, 2014, **128**, 398–402.
30 P. Galletto, P. F. Brevet, H. H. Girault, R. Antoine and M. Broyer, *Chem. Commun.*, 1999, 581–582.
31 J. Nappa, G. Revillod, J.-P. Abid, I. Russier-Antoine, C. Jonin, E. Benichou, H. H. Girault and P. F. Brevet, *Faraday Discuss.*, 2004, **125**, 145.
32 J. Nappa, G. Revillod, I. Russier-Antoine, E. Benichou, C. Jonin and P. F. Brevet, *Phys. Rev. B*, 2005, **71**, 165407.
33 N. Goubet, Y. Ding, M. Brust, Z. L. Wang and M.-P. Pileni, *ACS Nano*, 2009, **3**, 3622–3628.
34 T. Jain, F. Westerlund, E. Johnson, K. Moth-Poulsen and T. Bjørnholm, *ACS Nano*, 2009, **3**, 828–834.
35 Y. Wang, D. Wan, S. Xie, X. Xia, C. Z. Huang and Y. Xia, *ACS Nano*, 2013, **7**, 4586–4594.
36 T. Yi, R. Clément, C. Haut, L. Catala, T. Gacoin, N. Tancrez, I. Ledoux and J. Zyss, *Adv. Mater.*, 2005, **17**, 335–338.
37 H. Le Bozec, T. Le Bouder, O. Maury, A. Bondon, I. Ledoux, S. Deveau and J. Zyss, *Adv. Mater.*, 2001, **13**, 1677–1681.
38 Y. E. Harfouch, E. Benichou, F. Bertorelle, I. Russier-Antoine, C. Jonin, N. Lascoux and P. F. Brevet, *J. Phys. Condens. Matter*, 2012, **24**, 124104.
39 J. Napa, I. Russier-Antoine, E. Benichou, C. Jonin, P-F. Brevet, Chem. Phys. Lett., 2005, 415, 246-250.
40 P. B. Johnson and R. W. Christy, *Phys. Rev. B*, 1972, **6**, 4370–4379.

6 | *Phys. Chem. Chem. Phys.,* 2015, **00**, 0-0

This journal is © The Royal Society of Chemistry 20xx